UV-cured polysulfone-based membranes: Effect of co-solvent addition and evaporation process on membrane morphology and SRNF performance

Veysi Altun, Jean-Christophe Remigy, Ivo F.J. Vankelecom

▶ **To cite this version:**

HAL Id: hal-01882541
https://hal.science/hal-01882541

Submitted on 27 Sep 2018

UV-cured polysulfone-based membranes: Effect of co-solvent addition and evaporation process on membrane morphology and SRNF performance

Veysi Altun[a], Jean-Christophe Remigy[b], Ivo F.J. Vankelecom[a],[*]

[a] Centre for Surface Chemistry and Catalysis, Faculty of Bioengineering Sciences, KU Leuven, Celestijnenlaan 200F, PO Box 2461, 3001 Leuven, Belgium
[b] Université de Toulouse, INPT, US Laboratoire de Génie Chimique, 118 Route de Narbonne, F-31062 Toulouse, France

ABSTRACT

Membranes consisting of a semi-interpenetrating network of polysulfone (PSU) and cross-linked polyacrylate were synthesized via non-solvent induced phase inversion followed by UV-treatment. Tetrahydrofuran (THF) or 1,4-dioxane (DIO) was added as co-solvent to the *N,N*-dimethylformamide (DMF)-based polymer solutions and cast films were subjected to evaporation prior to coagulation. Effects of synthesis variables on the membrane morphology and solvent resistant nanofiltration (SRNF) performance were investigated by using a Rose Bengal solution in isopropanol. By increasing the evaporation time from 0 to 100 s for the membranes prepared with THF and DIO as co-solvent respectively, rejections increased from 65.3% to 94.2% and 60.1–89.1%, while permeances decreased from 0.29 to 0.01 l/m^2 h bar and 0.41–0.08 l/m^2 h bar. A similar effect was observed when the co-solvent/solvent ratio was increased from 0/100 to 100/0: rejections increased from 63.1% to 94.9% and 59.2–90.6%, while permeances decreased from 0.43 to 0.01 l/m^2 h bar for THF-based membranes and to 0.07 l/m^2 h bar for DIO-based membranes respectively. A post-treatment was performed to increase the flux by immersing UV-cured PSU-based films in DMF for 48 h. The resultant membranes showed higher permeances and lower rejections, making them especially useful as potential candidates for stable supports to apply selective layers upon, such as e.g. in thin film composite (TFC) membranes. As observed in scanning electron microscopy, higher evaporation times and lower initial co-solvent concentrations resulted in less or even no macrovoids.

1. Introduction

Polymeric membranes are extensively employed in gas and liquid separations due to their good processability and low cost [1–3]. These membranes mostly demonstrate an asymmetric structure and are fabricated via the phase inversion process where a polymer solution is cast on a support, followed by immersion in a non-solvent bath where polymer precipitation and membrane formation appears [4–11]. Solvent resistant nanofiltration (SRNF) is a contemporary process that allows the separation of organic mixtures down to a molecular level by applying a pressure gradient over a membrane [12,13]. It is entering as an innovative technology in petrochemical, food & beverage, pharmaceutical industries where organic solvent streams need to be treated. Besides permeability and selectivity, the chemical stability of the membranes is of great importance for such applications. In SRNF, both polymeric and inorganic membranes are used with molecular weight cut-offs in the range of 200–1000 Da [9,14–19].

Polysulfone (PSU) has strong thermal and mechanical properties which makes it an ideal candidate for broad membrane applications [20–25]. However, performance of these membranes and many others,

such as polyimide (PI) and polyether ketone, are still inadequate in the SRNF process because of their low resistance in aprotic solvents, such as *N*-methylpyrrolidone (NMP) and *N,N*-dimethylformamide (DMF) [26,27]. This problem can be solved by introducing cross-linking. The most common method to realize this is via chemical cross-linking [26,28–31]. However, it is less suitable for PSU due to its limited chemical reactivity. Additionally, chemical cross-linking generally requires a series of reaction steps which induce toxic contaminants such as diamines [26]. Therefore, radiation treatment via UV or electron beam (EB) can be a preferred alternative procedure for PSU [32–35]. The high cost and relative complexity of EB-curing units render UV-curing generally preferred [36]. Usually, surface modification of PSU-membranes is targeted via UV radiation to realize grafting [37,38]. Very recently, a simple and effective method was developed to depth-cure PSU-membranes via UV-curing [39]. In this approach, UV-irradiation was applied to PSU membrane films containing cross-linker and photo-initiator, prepared via non-solvent induced phase separation (NIPS) process. Combinations of various photo-initiators and cross-linkers were investigated to find a practically useful system [40,41]. As well-known, the final SRNF performance and membrane morphology

can be modified easily through even slight changes in synthesis protocol or composition of the casting solution. In-depth analysis of the phase inversion parameters is thus still necessary to achieve the best performance with UV-cured PSU-membranes via this method.

Among the most effective parameters to tune phase inversion parameters [9,42–46], evaporation time prior to immersion, choice of co-solvent and solvent/co-solvent ratio are easily accessible and well understood [41,46–52]. In present study, the influence of evaporation time and the role of co-solvent (tetrahydrofuran (THF) or 1,4-dioxane (DIO)) on the formation, performance and morphology of UV depth-cured PSU-based is thus investigated to further optimize this type of interesting membranes with respect to use in SRNF.

2. Experimental

2.1. Materials

Polysulfone (PSU) (Udel P-1700 LCD, Mn=21 000 g mol^{-1}) was kindly provided by Solvay (Belgium) and dried for 24 h at 100 °C prior to use. The polyethylene terephthalate non-woven fabric (PET Novatexx 2413) was kindly supplied by Freudenberg (Germany). Dipentaerythritol penta-acrylate (SR399LV, Sartomer) was used as cross-linker. 2,4,6-Trimethylbenzoyl-diphenyl-phosphine oxide was purchased from Sigma-Aldrich and used as photo-initiator. Table 1 shows details of photo-initiator and cross-linker used. Rose Bengal (RB) was obtained from Sigma-Aldrich. N,N-dimethylformamide (99.5%, DMF), tetrahydrofuran (99.5%, THF) and 1,4-dioxane (99%, DIO) were purchased from Acros and used as received.

2.2. Membrane synthesis

Two different series of membranes were prepared to determine the influence of evaporation time and the role of co-solvent as phase inversion parameters on the performance and morphology of the UV-cured PSU-membranes. In the first series, the influence of evaporation time was analyzed by using a DMF-based solution, with two different co-solvent (THF and DIO) with a ratio of DMF to co-solvent equal to 85/15. As evaporation times 0, 10, 20, 30, 60 or 100 s were used. It has to be mentioned that all membranes were evaporated for roughly about

5 s extra, which is the required time to move the cast film from the casting equipment to the coagulation bath. In the second series, the influence of co-solvent was analyzed by using a DMF (boiling point, 153 °C) based solution with the same THF (boiling point, 66 °C) and DIO (boiling point, 101 °C) as co-solvent keeping evaporation time constant (30 s), but with various ratios of DMF to these co-solvents: 100/0, 75/25, 50/50, 25/75 and 0/100. All samples were prepared at room temperature under the atmospheric pressure. In both series, the polymer concentration was kept constant at 21 wt%. Cross-linker and photo-initiator were used at 5 wt% and 3 wt%, respectively. After obtaining a homogenous polymer solution, membranes with a wet thickness of 200 µm were cast at a speed of 1.81 m/min onto a glass plate or a polypropylene/polyethylene non-woven fabric (Novatexx 2413) impregnated with DMF. Before immersion into the coagulation bath, the membrane was kept in ambient air for a certain time. The membranes were stored in distilled water prior to the UV treatment.

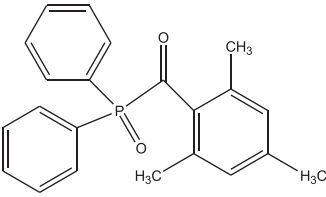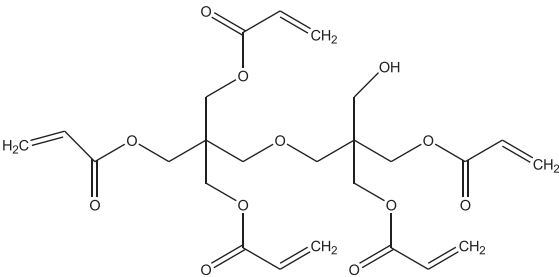### 2.3. UV-curing of asymmetric PSU-based membranes

The PSU-based membranes were passed through a UV-curing set up (UVAPrintS200, HonleUV France) on a conveyor belt at a line speed of 10 m/min. UVA (320–390 nm) was used as the main irradiation light. According to our previous study [39], the dose of energy to cure the membranes was chosen as 5 J/cm^2.

To increase the flexibility and prevent pore collapse for better filtration, some of the cross-linked PSU-membranes were impregnated after the UV-curing. The membranes were stored in a solution including 40% (v/v) of glycerol and 60% (v/v) of propan-2-ol for 48 h at room temperature, and subsequently air-dried. ATR-FTIR and SEM were performed to non-impregnated UV-cured PSU-membranes.

2.4. Viscosity measurements

Viscosity measurements were carried out with an Anton Paar MCR501 rheometer with a cone-plane geometry with solvent trap at 20 °C. The polymer solution was loaded onto the plate, and the cone was lowered onto the sample. It was then covered by a lid to avoid solvent evaporation. The sample temperature was controlled by a Peltier element with high accuracy. Viscosity at different shear rates

Table 1
Photo-initiator and cross-linker used in this study.

Name	MW (gmol^{-1})	Structure
2,4,6-Trimethylbenzoyl-diphenyl-phosphine oxide (Darocur™ TPO)	348	
Dipenta-erythritol penta-acrylate (Sartomer™ SR399LV)	524	

was measured in steady-shear flow from 0.01 to 100 1/s. Data acquisition and analysis was done using RheoPlus software (Anton Paar GmbH, Austria).

2.5. Scanning electron microscopy (SEM)

Philips XL30 FEG scanning electron microscope has been employed to obtain membrane cross-section images. The membrane samples were freeze-cracked in liquid nitrogen. To reduce sample charging under the electron beam, samples were coated with a 1.5–2 nm gold layer using a Cressington HR208 high-resolution sputter coater.

2.6. Solubility parameters

The Hansen solubility parameters (HSP) are useful to check the solvent strength and the solubility of polymer. Based on the thermodynamics of the solubility equilibrium, Hansen calculated the enthalpy of miscibility using the three Hansen solubility parameters of the solvent and polymer. This HSP δ_D, δ_P, and δ_H are the partial HSP attributed to dispersive forces, polar forces, and hydrogen bonding, respectively. Thus the HSP are properties of a polymer or a solvent. The total solubility parameter δ is the geometric mean of the three components given by the following equation [53]

$$\delta = (\delta_D{}^2 + \delta_P{}^2 + \delta_H{}^2)^{1/2} \tag{1}$$

The three partial HSP are used to define a space where the solubility volume (modelled as a sphere of radius R0 and center δ_D, δ_P, and δ_H of polymer) a polymer is plotted. This solubility volume includes of the solvents of a polymer and Ro is also called the critical radius of interaction of a polymer. A solubility parameter distance (Ra) is a measure of affinities between polymer (1) and solvent (2) and is based on their individual Hansen solubility parameters by the following equation;

$$Ra = [4(\delta_{D2} - \delta_{D1})^2 + 4(\delta_{P2} - \delta_{P1})^2 + 4(\delta_{H2} - \delta_{H1})^2]^{1/2} \tag{2}$$

The relative energy difference, RED, is equal to Ra/R0. Solubility of the polymer in the solvent is expected in case of RED value is smaller than 1. Solubility increases when the RED value is below 1.

2.7. Swelling/solvent resistance test

The solvent resistance of prepared and cured PSU-membranes was analyzed by visual inspection after keeping membrane samples in various solvents at room temperature for at least 24 h.

2.8. Filtration Experiments

Filtrations were performed in a dead-end filtration cell with a high throughput filtration module (High Throughput Membrane Systems Leuven, Belgium) [12,54], at room temperature and under pressures ranging from 10 to 30 bar allowing for simultaneous filtrations of 16 membranes. Membrane samples were placed in the module and sealed with Viton® O-rings. The active membrane surface area was 0.000452 m^2. A solution of 17.5 µM Rose Bengal (1017 Da) in propanol (IPA) was used as feed. It was stirred magnetically at 350 rpm to reduce concentration polarization. Permeances, expressed in (l/m^2 h bar), were determined gravimetrically by weighing the collected permeate. Rejections (R, %) were defined as $(1-C_p/C_f) \times 100$, where C_f and C_p denote the dye concentrations in the initial feed and in the permeate respectively. Dye concentrations were recorded on a Perkin-Elmer Lambda 12 UV−vis spectrophotometer at a wavelength of 555 nm. Filtration measurements lasted an average 20 h and 4 membrane coupons were tested for each membrane sample. Typically 3 samples were taken for analysis per coupon after having reached

steady state conditions.

2.9. Post-treatment of UV-cured PSU-based membranes with immersion in DMF

A solvent activation post-treatment step was performed on a selection of UV-cured membranes in order to increase the solvent flux according to Solomon et al. [65]. Selected membranes were immersed in DMF for 48 h. The performance of treated membranes was evaluated
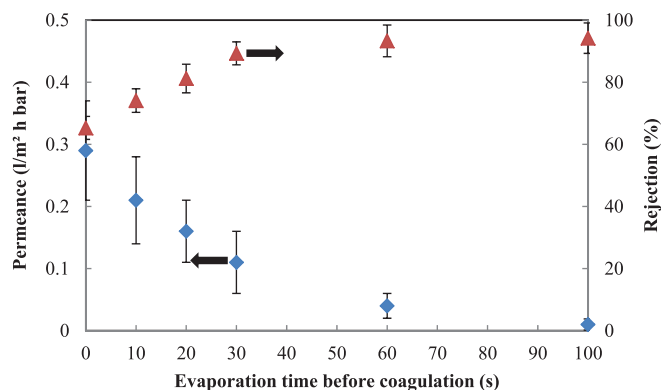

Fig. 1. Effect of evaporation time on the separation performance of the UV-cured PSU/THF-based membranes with a THF/DMF ratio of [15/85], in terms of rejection and permeance for a RB/IPA feed. Permeance is indicated as blue diamonds and rejection as red triangles. (For interpretation of the references to color in this figure legend, the reader is referred to the web version of this article.)

Fig. 2. Effect of evaporation time on the separation performance of the UV-cured PSU/DIO-based membranes with DIO/DMF ratio of [15/85], in terms of rejection and permeance for a RB/IPA feed. Permeance is indicated as blue diamonds and rejection as red triangles. (For interpretation of the references to color in this figure legend, the reader is referred to the web version of this article.)
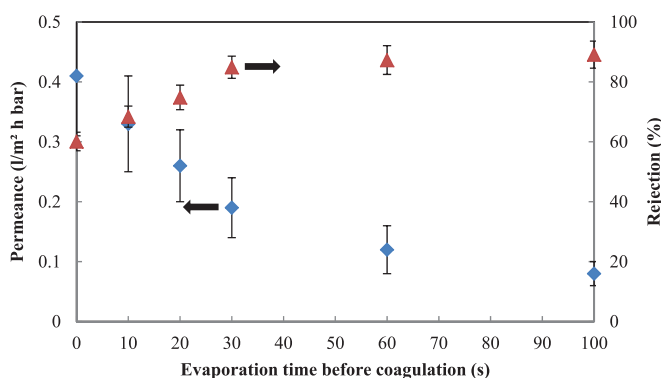

Fig. 3. Effect of evaporation time on the weight loss of the PSU/DMF/DIO and PSU/DMF/THF cast films with co-solvent/solvent ratios of [15/85]. THF is indicated as blue diamonds and DIO as red squares. (For interpretation of the references to color in this figure legend, the reader is referred to the web version of this article.)

Fig. 4. Effect of evaporation time on the morphology of the UV-Cured PSU-membranes: a-f: THF; g-l: DIO containing membranes with [15/85] co-solvent/solvent ratio (0, 10, 15 , 20 , 30 , 60 and 100 s respectively).

through filtrations using IPA/RB and DMF/RB as feed solutions.

3. Results and discussion

3.1. Influence of evaporation time

3.1.1. Filtration performance

In the membrane fabrication process, an evaporation step is frequently applied to get a more dense membrane surface layer when the casting solution includes volatile (co-)solvents [42,46,50]. Consequently, a thin layer is created at the surface of the cast film with a locally increased polymer concentration. The formed layer acts as a resistance barrier between the deeper membrane regions and the coagulation bath, leading to delayed demixing [55,56]. Longer evaporation times remove more co-solvent from the surface of the cast film, thus the region with increased polymer concentration at the top of the film enlarges and turns into a more concentrated nascent skin layer [49,50]. Consequently, asymmetric membranes with a dense and thick skin layer are formed and with less chances for macrovoid creation.

Literature with respect to SRNF-membranes is in this respect not unambiguous however. For a certain type of PI-SRNF membrane (Matrimid - NMP - THF), a longer evaporation time (0–120 s) increased rejections and decreased permeances [50], while moderate evaporation (0–40 s) of a volatile solvent before the immersion in a coagulation bath was found needless to create a selective skin layer in another PI-system (P84 - DMF - DIO) [47]. For PSU-based SRNF

Fig. 5. Effect of co-solvent/solvent ratio (THF/DMF) on the separation performance of the UV-cured PSU-membranes given 30 s of evaporation time. Permeance is indicated as blue diamonds and rejection as red triangles. (For interpretation of the references to color in this figure legend, the reader is referred to the web version of this article.)
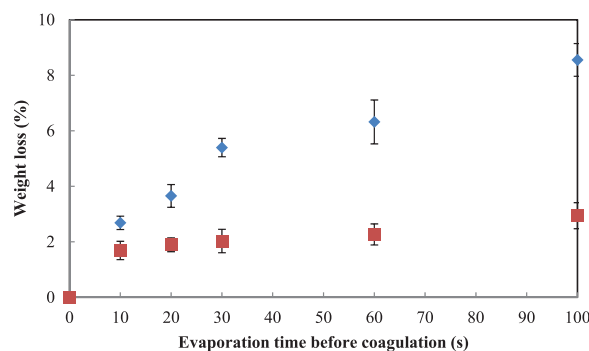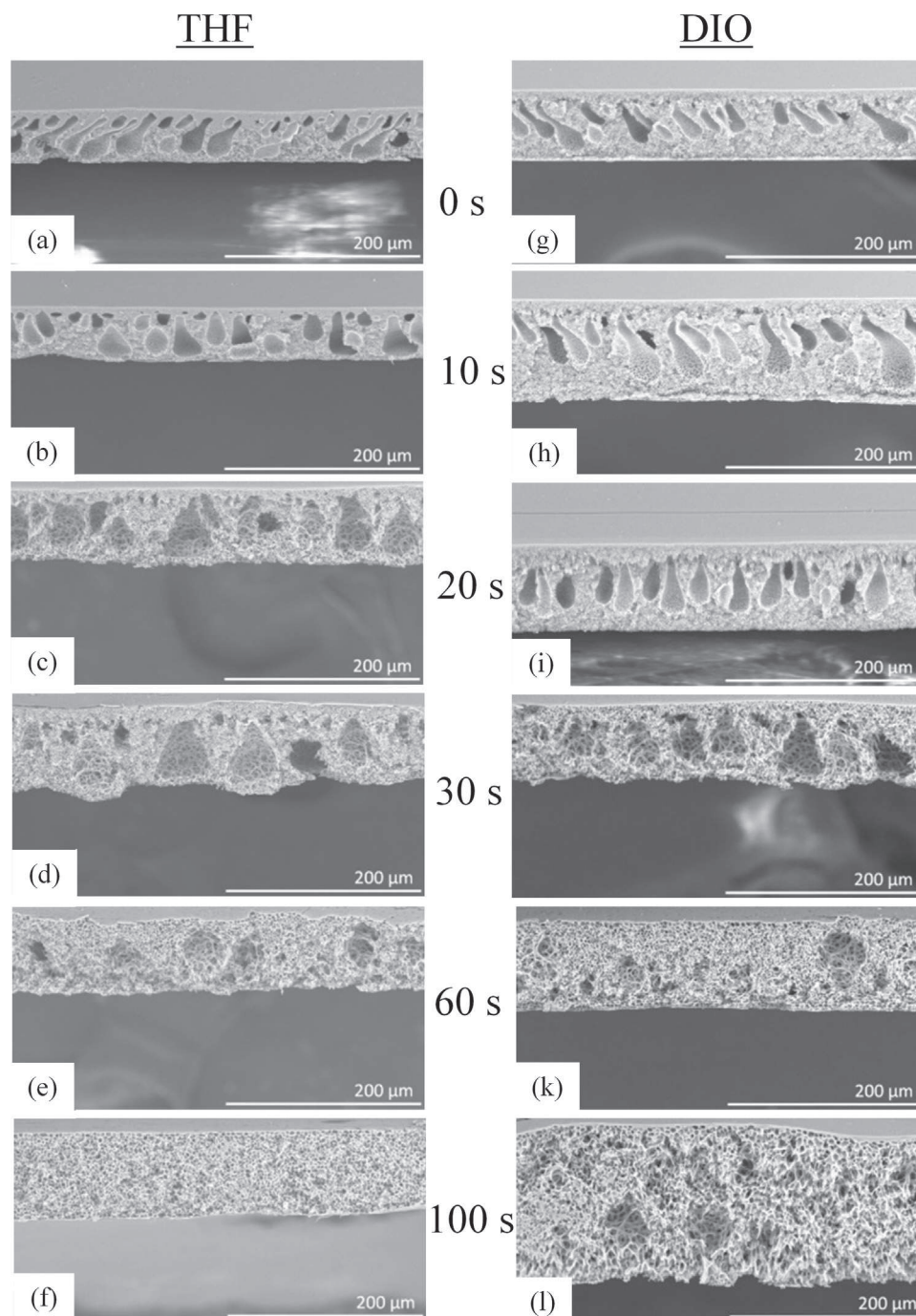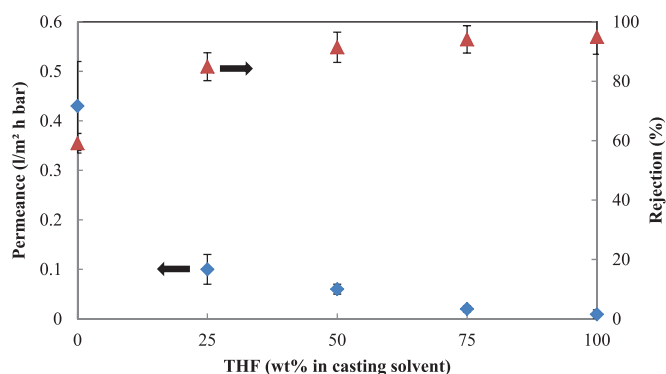

Fig. 6. Effect of co-solvent/solvent ratio (DIO/DMF) on the separation performance of the UV-cured PSU-membranes given 30 s of evaporation time. Permeance is indicated as blue diamonds and rejection as red triangles. (For interpretation of the references to color in this figure legend, the reader is referred to the web version of this article.)
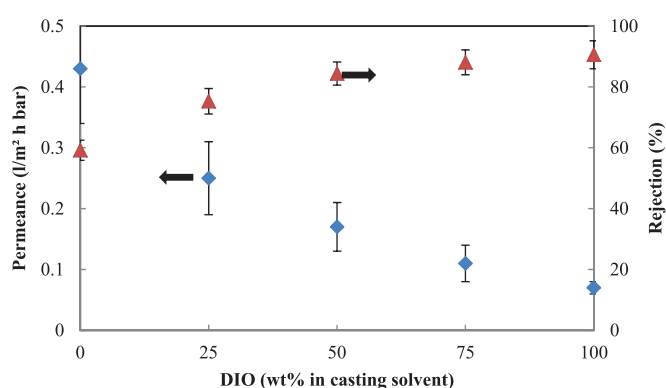
membranes, an increased evaporation time caused a continuous decline in permeance while it took the rejection to a certain ultimate level [46].

Six different evaporation times of 0, 10, 20, 30, 60 or 100 s were allocated for evaporation of THF and DIO before immersion of the cast films in the water bath. As seen from Fig. 1, increasing the evaporation time changes the membrane performance most notably for THF series. The flux of IPA decreased from 0.29 to 0.01 l/m^2 h bar, while the RB retention increased from 65.3% to 94.2% by increasing the evaporation time from 0 to 100 s. Additionally, rejections increased distinctly till an evaporation time of 30 s to a maximum value of 89.3%, while IPA permeances further decreased continuously with evaporation time. The ideal time for evaporation of THF as co-solvent before immersion in the precipitation bath can thus be assumed to be around 30 s as beyond 30 s, rejection stayed almost constant but permeance dropped down to zero.

For DIO containing membranes, the flux of IPA decreased from 0.41 to 0.08 l/m^2 h bar while RB retention increased from 60.1% to 89.1% by increasing the evaporation time from 0 to 100 s (Fig. 2). Similar to THF-based membranes, 30 s seemed to be the optimum evaporation time to apply for DIO-based membranes, as RB rejections were then close to the maximum value.

In general, THF containing membranes showed lower permeance and higher rejection for each applied evaporation time due to the faster THF evaporation rate arising out of lower boiling point (Fig. 1).

Additionally, the weight loss of the DIO and THF-containing cast films was measured as a function of evaporation time. THF-containing films lost more weight compared to DIO-containing films (Fig. 3), as a consequence of the low boiling point of THF.

3.1.2. Morphology

Membrane morphology is notably influenced by changing evaporation time, as demonstrated in the SEM pictures (Fig. 4). For both co-solvents used, the number of macrovoids under the skin layer decreased by increasing the evaporation time. Their size also decreased, and the macrovoids finally even fully disappeared at the longest evaporation times (100 s). This can all be related to the delayed demixing induced by creating a tougher mass transfer barrier during the evaporation step.

3.2. Influence of co-solvent type

3.2.1. Filtration performance

Many studies showed that the addition of a co-solvent to casting solutions could significantly influence the performance and morphology of asymmetric membranes for [47,50,56].

Figs. 5 and 6 show the effect of co-solvent/solvent ratio (THF/DMF and DIO/DMF respectively) on the separation performance of UV-cured PSU membranes. THF was expected to evaporate well during the evaporation step because of its low boiling point. Fig. 5 shows that increasing the THF/DMF weight ratio induced lower IPA permeances and higher RB rejections due to the densification of the membranes. The membranes prepared from solutions containing DIO as co-solvent showed a similar behavior as the THF-based membranes: IPA permeance decreases continuously while the RB rejection increases distinctly till a certain ratio, and then further remains rather stable with increasing DIO/DMF ratio (Fig. 6). It can be seen that THF-based membranes have lower permeance than DIO-based membranes at the same co-solvent/solvent ratio. This can be explained by the higher volatility of THF compared to DIO which leads to formation of a denser skin layer at a certain evaporation time due to the loss of more co-solvent, as earlier mentioned in the discussion of the evaporation time. Varying the THF/DMF and DIO/DMF ratio in the casting solution showed us that it is possible to have a higher rejection with optimum ratio, but permeance stayed too low in all cases to become satisfactory (> 1/l m^2 h bar) for SRNF-applications [57].

3.2.2. Morphology

By increasing the THF/DMF and DIO/DMF weight ratios from 0/100 to 100/0 in the casting solutions, finger-like macrovoids appeared in Fig. 7[58]. The solvent/non-solvent exchange rate is lowered after the formation of a dense top layer on top of the cast polymer film which slows down the demixing deeper in the membrane. Therefore, macrovoids have longer time to be formed and grow in size in membrane with a higher THF concentration [40,59].

3.2.3. Viscosity change

Apart from thermodynamics, the kinetic aspects of the phase inversion process also affect the membrane formation process. The viscosity of the casting solution can be changed by adding co-solvent which alters the phase inversion process in terms of a slower diffusion of solvent into the non-solvent bath and of non-solvent into the polymer film. Fig. 8 demonstrates the change in viscosity upon addition of co-solvent to the casting solution. The viscosity of the polymer solution is mainly fixed by the quality of the solvent. Dissolution of polymer is easier in the presence of a solvent of high affinity. In a *good* solvent, polymer chains stretches where as in a *poor* solvent the polymer chain collapses. As a result of the stretched chains, polymer solution becomes more viscous [60]. According to HSP interaction distance (Table 4), it can be estimated that DIO (5.4 MPa$^{1/2}$) is better solvent than THF (6.4 MPa$^{1/2}$) for PSU. Thus, in studied systems, the addition of DIO leads higher viscosity than addition of THF. The viscosity values presented in Fig. 7 are rather just indicative, since it was hard to perform the precise measurements, especially for the samples containing THF, due to the partial solidification caused by fast evaporation during the actual viscosity measurements. Nevertheless, it
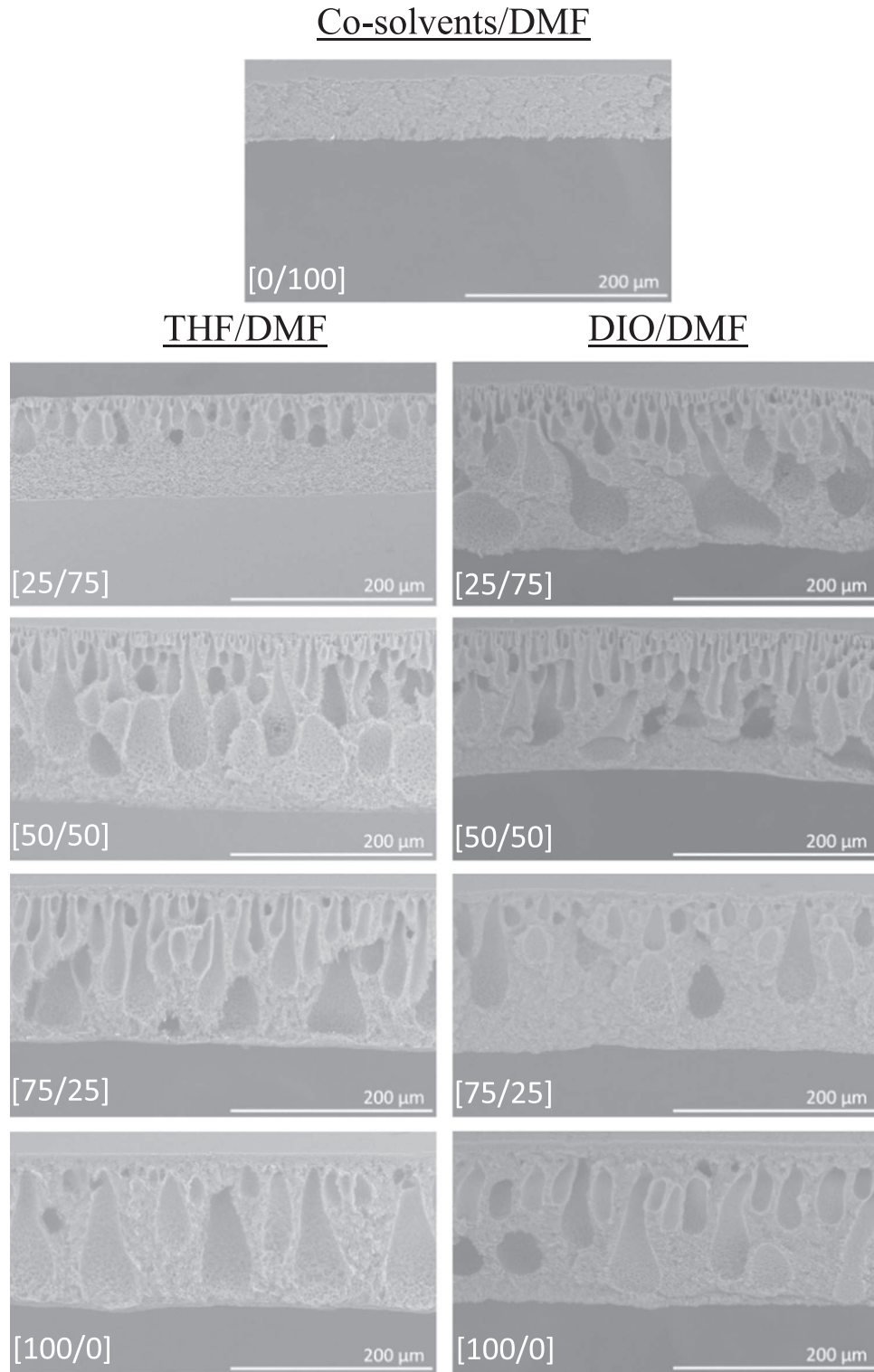
Co-solvents/DMF

[0/100]

THF/DMF

DIO/DMF

[25/75]

[25/75]

[50/50]

[50/50]

[75/25]

[75/25]

[100/0]

[100/0]

Fig. 7. Effect of co-solvent/solvent ratio on the morphology of the UV-cured PSU-membranes given 30 s of evaporation time.

is clear that addition of THF decreased the viscosity of the polymer solutions, while the addition of DIO increased the viscosity. Macrovoid formation is accepted to be suppressed by increasing the casting solution viscosity as demixing becomes more delayed [61,62]. Fig. 7 confirms this, since macrovoids disappeared when viscosity increased with higher DIO concentration, while they became more apparent when viscosity decreased at higher THF levels. However, increasing the co-solvent amount showed the same tendency in separation performance for both membranes. This thus proves that flux and rejection are controlled by the skin layer and that existence of macrovoids is not the dominating factor for the performance of these SRNF-membranes under the applied filtration conditions [63].

3.3. Solvent activation of UV-cured PSU membranes by immersion in DMF

To further evaluate the solvent stability and to increase the SRNF flux, UV-cured membranes were immersed in DMF for 48 h [64,65].
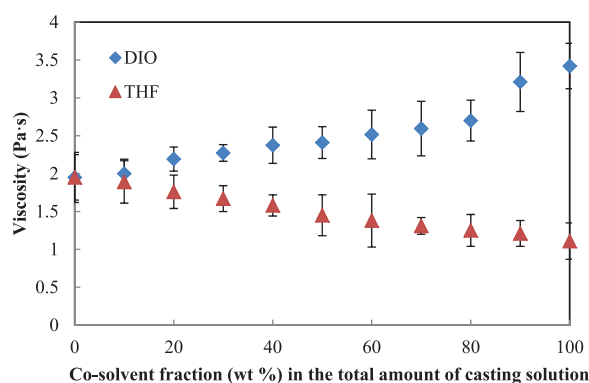
Fig. 8. Effect of co-solvent/solvent ratio concentration on the viscosity of the casting solutions of the UV-cured PSU-membranes (21 wt%).

Table 2
Properties of UV-cured PSU membranes that were selected for the immersion in DMF. Permeance column indicates the IPA/RB filtration results obtained before immersion in DMF.

Membrane	Co-solvent	Evaporation time (s)	Co-solvent/solvent (wt/wt)	Permeance
M1	THF	0	85/15	highest
M2	THF	30	100/0	lowest
M3	DIO	0	85/15	highest
M4	DIO	30	100/0	lowest

Table 3
The physico-chemical properties of the solvents used in the filtrations.

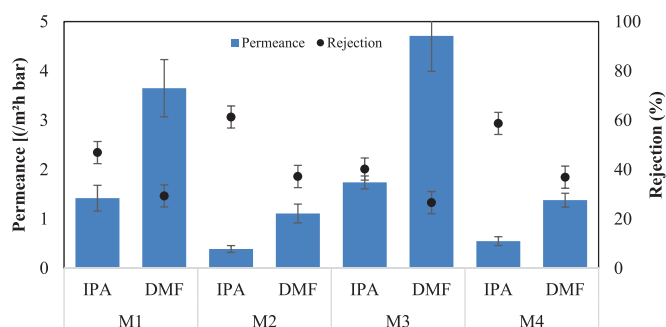| Solvents	Molar volume (cm^3/mol)	Viscosity (cP)	Molar volume/viscosity (cm^3/mol cP)
IPA	76.46	2.00	38.46
DMF	77.43	0.82	94.43

Fig. 9. Filtration performance of UV-cured membranes for RB in IPA and in DMF after solvent activation by immersion in DMF for 48 h. The composition of membranes (M1-M4) is given in Table 2.

The membranes with highest and lowest permeances were selected to check the effects of the DMF immersion (Table 2). The performances were measured first in IPA/RB to see the improvement in flux. Afterwards, the same membranes were tested in DMF/RB solution, which is a feed that would normally dissolve PSU membranes immediately. Table 3 demonstrates the physico-chemical properties of the solvents used in filtrations. As shown in Fig. 9, the IPA permeances increased distinctly compared to the results summarized in Table 2 (factors of 3–4) upon the treatment, while RB rejections decreased. Higher permeances were systematically observed for thr DMF/RB filtration, as commonly observed in previous studies [64,65]. The membranes stayed stable despite the decreasing selectivity).

Table 4
Solvent stability of the reference (without photoinitator and cross-linker) and UV-cured (5j/cm^2) PSU (21%wt) membranes with interaction distance (Ra) of solvents used.

Solvent	Reference	UV-cured	Interaction distance solvent /PSU (MPa$^{1/2}$)
IPA	0	0	11.5
Toluene	1	0	9.9
Xylene mixture	1	0	9.7
Butyl acetate	X	0	9.3
Acetone	X	0	8.8
DMF	1	X	7.7
THF	1	X	6.4
NMP	1	X	5.4

0-stable, X-swelling, 1-dissolution.

3.4. Solvent stability

The reference and UV-cured membranes were immersed in various solvents commonly used in processing, to prove the efficiency of UV treatment with respect to solvent stability. Table 4 shows the solvent stability of the reference and cured membranes with calculated HSP interaction distance of various solvents used for stability experiment. As expected, all membranes were stable in IPA. The reference membrane swelled after immersion in butyl acetate and acetone, while the UV-cured PSU membrane remained unaltered in these solvents. The reference membrane dissolved in toluene and xylene, while the UV-cured PSU membrane was stable and hardly swelled. After immersion in DMF, THF and NMP, the reference membrane dissolved completely while the UV-cured PSU membrane swelled slightly here, but without dissolving. Regarding the outcome of the solvent stability test and the HSP interaction distance, it can be concluded that the cross-linked membranes could be used with solvents having an interaction distance higher than 8.8 safely (no swelling). However, this hypothesis seems invalid for two outlier solvents, since the reference membrane dissolves in toluene and xylene mixtures (interaction distance > 8.8). This could be attributed to π-interactions between PSU and aromatic solvents which are not properly taken in account in calculation of HSP. Furthermore, the reference membrane just swells in aliphatic solvents such as acetone and butyl acetate. As a result, it was monitored that the UV irradiation distinctly improved the solvent stability of the PSU-based membranes.

4. Conclusions

This study describes the effects of phase inversion parameters on a UV-cured PSU system for the fabrication of SRNF-membranes via NIPS. Co-solvent content and evaporation time before immersion into non-solvent bath were selected as parameters to tune the separation performance of the membranes. Longer evaporation times before coagulation of a cast membranes consistently decreased the permeance till 0.01 and 0.08 l/m^2 h bar (at 100 s) for the membranes containing co-solvent THF and DIO as respectively. Meanwhile, the rejection of the same membranes increased to 89.3% (THF-based) and 84.9% (DIO-based) till evaporation times around 30 s and then remained almost constant when further extending the evaporation process. Too long evaporation times (> 30 s) should thus be avoided.

When adding a more volatile co-solvent to the casting solutions, permeances steadily declined to 0.01 and 0.07 l/m^2 h bar and rejections increased to 94.9% and 90.6% for the membranes containing co-solvent THF and DIO as respectively. The morphology of the prepared membranes was affected strongly by the phase inversion parameters. The appearance of finger-like macrovoids could be explained via viscosity changes in the casting solution when co-solvent was added. An increase in evaporation times to 100 s reduced macrovoid formation with appearance of spongy structures, ascribed to the formation of

a more concentrated polymer layer on top of the cast membranes at extended evaporation times. Finally, post-treatment with DMF significantly improved the permeances but reduced rejections. These membranes could still be useful as support layer in TFC membrane preparation processes.

Acknowledgements

References

[1] S. Basu, A.L. Khan, A. Cano-Odena, C. Liu, I.F.J. Vankelecom, Membrane-based technologies for biogas separations, Chem. Soc. Rev. 39 (2010) 750–768.

[2] A.F. Ismail, L.P. Yean, Review on the development of defect-free and ultrathin-skinned asymmetric membranes for gas separation through manipulation of phase inversion and rheological factors, J. Appl. Polym. Sci. 88 (2003) 442–451.

[3] S. Hermans, H. Mariën, C. Van Goethem, I.F.J. Vankelecom, Recent developments in thin film (nano)composite membranes for solvent resistant nanofiltration, Curr. Opin. Chem. Eng. 8 (2015) 45–54.

[4] C. Klaysom, T.Y. Cath, T. Depuydt, I.F.J. Vankelecom, Forward and pressure retarded osmosis: potential solutions for global challenges in energy and water supply, Chem. Soc. Rev. 42 (2013) 6959–6989.

[5] B.D. Coday, B.G.M. Yaffe, P. Xu, T.Y. Cath, Rejection of trace organic compounds by forward osmosis membranes: a literature review, Environ. Sci. Technol. 48 (2014) 3612–3624.

[6] X. Feng, R.Y.M. Huang, Liquid separation by membrane pervaporation: a review, Ind. Eng. Chem. Res. 36 (1997) 1048–1066.

[7] R.-C. Ruaan, T. Chang, D.-M. Wang, Selection criteria for solvent and coagulation medium in view of macrovoid formation in the wet phase inversion process, J. Polym. Sci. Part B: Polym. Phys. 37 (1999) 1495–1502.

[8] S. Perez, E. Merlene, E. Robert, J.P.C. Addad, A. Viallat, Characterization of the surface layer of integrally skinned polyimide membranes: relationship with their mechanism of formation, J. Appl. Polym. Sci. 47 (1993) 1621–1631.

[9] A.K. Hołda, I.F.J. Vankelecom, Understanding and guiding the phase inversion process for synthesis of solvent resistant nanofiltration membranes, J. Appl. Polym. Sci. 132 (2015) 42130–42147.

[10] G.R. Guillen, Y. Pan, M. Li, E.M.V. Hoek, Preparation and characterization of membranes formed by nonsolvent induced phase separation: a review, Ind. Eng. Chem. Res. 50 (2011) 3798–3817.

[11] S. Hermans, R. Bernstein, A. Volodin, I.F.J. Vankelecom, Study of synthesis parameters and active layer morphology of interfacially polymerized polyamide–polysulfone membranes, React. Funct. Polym. 86 (2015) 199–208.

[12] P. Vandezande, L.E.M. Gevers, J.S. Paul, I.F.J. Vankelecom, P.A. Jacobs, High throughput screening for rapid development of membranes and membrane processes, J. Membr. Sci. 250 (2005) 305–310.

[13] P. Marchetti, M.F. Jimenez Solomon, G. Szekely, A.G. Livingston, Molecular separation with organic solvent nanofiltration: a critical review, Chem. Rev. 114 (2014) 10735–10806.

[14] X. Li, S. De Feyter, I.F.J. Vankelecom, Poly(sulfone)/sulfonated poly(ether ether ketone) blend membranes: morphology study and application in the filtration of alcohol based feeds, J. Membr. Sci. 324 (2008) 67–75.

[15] A.V. Volkov, S.E. Tsarkov, A.B. Gilman, V.S. Khotimsky, V.I. Roldughin, V.V. Volkov, Surface modification of PTMSP membranes by plasma treatment: asymmetry of transport in organic solvent nanofiltration, Adv. Colloid Interface Sci. 222 (2015) 716–727.

[16] L.E.M. Gevers, G. Meyen, K. De Smet, P. Van De Velde, F. Du Prez, I.F.J. Vankelecom, P.A. Jacobs, Physico-chemical interpretation of the SRNF transport mechanism for solutes through dense silicone membranes, J. Membr. Sci. 274 (2006) 173–182.

[17] D. Bhanushali, S. Kloos, D. Bhattacharyya, Solute transport in solvent-resistant nanofiltration membranes for non-aqueous systems: experimental results and the role of solute–solvent coupling, J. Membr. Sci. 208 (2002) 343–359.

[18] S. Aerts, H. Weyten, A. Buekenhoudt, L.E.M. Gevers, I.F.J. Vankelecom, P.A. Jacobs, Recycling of the homogeneous Co-Jacobsen catalyst through solvent-resistent nanofiltration (SRNF), Chem. Commun. (2004) 710–711.

[19] D. Fritsch, P. Merten, K. Heinrich, M. Lazar, M. Priske, High performance organic solvent nanofiltration membranes: development and thorough testing of thin film composite membranes made of polymers of intrinsic microporosity (PIMs), J. Membr. Sci., 401–402 (2012) 222–231.

[20] K. Majewska-Nowak, Synthesis and properties of polysulfone membranes, Desalination 71 (1989) 83–95.

[21] A.K. Hołda, I.F.J. Vankelecom, Integrally skinned PSf-based SRNF-membranes prepared via phase inversion—Part A: influence of high molecular weight additives, J. Membr. Sci. 450 (2014) 512–521.

[22] J.Y. Park, M.H. Acar, A. Akthakul, W. Kuhlman, A.M. Mayes, Polysulfone-graft-poly(ethylene glycol) graft copolymers for surface modification of polysulfone

[23] membranes, Biomaterials 27 (2006) 856–865.

[24] A.K. Hołda, I.F.J. Vankelecom, Integrally skinned PSf-based SRNF-membranes prepared via phase inversion—Part B: influence of low molecular weight additives, J. Membr. Sci. 450 (2014) 499–511.

[24] H. Yu, Y. Cao, G. Kang, J. Liu, M. Li, Q. Yuan, Enhancing antifouling property of polysulfone ultrafiltration membrane by grafting zwitterionic copolymer via UV-initiated polymerization, J. Membr. Sci. 342 (2009) 6–13.

[25] E. Eren, A. Sarihan, B. Eren, H. Gumus, F.O. Kocak, Preparation, characterization and performance enhancement of polysulfone ultrafiltration membrane using PBI as hydrophilic modifier, J. Membr. Sci. 475 (2015) 1–8.

[26] K. Vanherck, G. Koeckelberghs, I.F.J. Vankelecom, Crosslinking polyimides for membrane applications: a review, Prog. Polym. Sci. 38 (2013) 874–896.

[27] H. Ohya, I. Okazaki, M. Aihara, S. Tanisho, Y. Negishi, Study on molecular weight cut-off performance of asymmetric aromatic polyimide membrane, J. Membr. Sci. 123 (1997) 143–147.

[28] Y.H. See Toh, F.W. Lim, A.G. Livingston, Polymeric membranes for nanofiltration in polar aprotic solvents, J. Membr. Sci. 301 (2007) 3–10.

[29] K. Hendrix, K. Vanherck, I.F.J. Vankelecom, Optimization of solvent resistant nanofiltration membranes prepared by the in-situ diamine crosslinking method, J. Membr. Sci. 421–422 (2012) 15–24.

[30] I.B. Valtcheva, P. Marchetti, A.G. Livingston, Crosslinked polybenzimidazole membranes for organic solvent nanofiltration (OSN): analysis of crosslinking reaction mechanism and effects of reaction parameters, J. Membr. Sci. 493 (2015) 568–579.

[31] K. Vanherck, A. Cano-Odena, G. Koeckelberghs, T. Dedroog, I. Vankelecom, A simplified diamine crosslinking method for PI nanofiltration membranes, J. Membr. Sci. 353 (2010) 135–143.

[32] M. Stephan, D. Pospiech, R. Heidel, T. Hoffmann, D. Voigt, H. Dorschner, Electron beam irradiation of molten polysulfone, Polym. Degrad. Stab. 90 (2005) 379–385.

[33] A. Schulze, B. Marquardt, S. Kaczmarek, R. Schubert, A. Prager, M.R. Buchmeiser, Electron Beam-Based Functionalization of Poly(ethersulfone) Membranes, Macromol. Rapid Commun. 31 (2010) 467–472.

[34] H. Yamagishi, J.V. Crivello, G. Belfort, Development of a novel photochemical technique for modifying poly (arylsulfone) ultrafiltration membranes, J. Membr. Sci. 105 (1995) 237–247.

[35] V. Altun, M. Bielmann, I.F.J. Vankelecom, EB depth-curing as a facile method to prepare highly stable membranes, RSC Adv. 6 (2016) 55526–55533.

[36] D. He, H. Susanto, M. Ulbricht, Photo-irradiation for preparation, modification and stimulation of polymeric membranes, Prog. Polym. Sci. 34 (2009) 62–98.

[37] J. Pieracci, J.V. Crivello, G. Belfort, Photochemical modification of 10 kDa polyethersulfone ultrafiltration membranes for reduction of biofouling, J. Membr. Sci. 156 (1999) 223–240.

[38] H. Yamagishi, J.V. Crivello, G. Belfort, Evaluation of photochemically modified poly (arylsulfone) ultrafiltration membranes, J. Membr. Sci. 105 (1995) 249–259.

[39] I. Struzynska-Piron, J. Loccufier, L. Vanmaele, I.F.J. Vankelecom, Synthesis of solvent stable polymeric membranes via UV depth-curing, Chem. Commun. 49 (2013) 11494–11496.

[40] I. Strużyńska-Piron, J. Loccufier, L. Vanmaele, I.F.J. Vankelecom, Parameter study on the preparation of UV depth-cured chemically resistant polysulfone-based membranes, Macromol. Chem. Phys. 215 (2014) 614–623.

[41] I. Strużyńska-Piron, M.R. Bilad, J. Loccufier, L. Vanmaele, I.F.J. Vankelecom, Influence of UV curing on morphology and performance of polysulfone membranes containing acrylates, J. Membr. Sci. 462 (2014) 17–27.

[42] K. Hendrix, G. Koeckelberghs, I.F.J. Vankelecom, Study of phase inversion parameters for PEEK-based nanofiltration membranes, J. Membr. Sci. 452 (2014) 241–252.

[43] H. Yanagishita, T. Nakane, H. Yoshitome, Selection criteria for solvent and gelation medium in the phase inversion process, J. Membr. Sci. 89 (1994) 215–221.

[44] K. Hendrix, M. Vaneynde, G. Koeckelberghs, I.F.J. Vankelecom, Synthesis of modified poly(ether ether ketone) polymer for the preparation of ultrafiltration and nanofiltration membranes via phase inversion, J. Membr. Sci. 447 (2013) 96–106.

[45] J. Ren, R. Wang, T.-S. Chung, D.F. Li, Y. Liu, The effects of chemical modifications on morphology and performance of 6FDA-ODA/NDA hollow fiber membranes for CO 2/CH 4 separation, J. Membr. Sci. 222 (2003) 133–147.

[46] A.K. Hołda, B. Aernouts, W. Saeys, I.F.J. Vankelecom, Study of polymer concentration and evaporation time as phase inversion parameters for polysulfone-based SRNF membranes, J. Membr. Sci. 442 (2013) 196–205.

[47] I. Soroko, M. Makowski, F. Spill, A. Livingston, The effect of membrane formation parameters on performance of polyimide membranes for organic solvent nanofiltration (OSN). Part B: analysis of evaporation step and the role of a co-solvent, J. Membr. Sci. 381 (2011) 163–171.

[48] N. Leblanc, D. Le Cerf, C. Chappey, D. Langevin, M. Métayer, G. Muller, Polyimide asymmetric membranes: elaboration, morphology, and gas permeation performance, J. Appl. Polym. Sci. 89 (2003) 1838–1848.

[49] F.G. Paulsen, S.S. Shojaie, W.B. Krantz, Effect of evaporation step on macrovoid formation in wet-cast polymeric membranes, J. Membr. Sci. 91 (1994) 265–282.

[50] P. Vandezande, X. Li, L.E.M. Gevers, I.F.J. Vankelecom, High throughput study of phase inversion parameters for polyimide-based SRNF membranes, J. Membr. Sci. 330 (2009) 307–318.

[51] V. Altun, M. Bielmann, I.F.J. Vankelecom, Study of phase inversion parameters for EB-cured PSU-based membranes, RSC Adv. 6 (2016) 110916–110921.

[52] I. Soroko, M. Sairam, A.G. Livingston, The effect of membrane formation parameters on performance of polyimide membranes for organic solvent nanofiltration (OSN). Part C. Effect of polyimide characteristics, J. Membr. Sci. 381 (2011) 172–182.

[53] C.M.Hansen, Hansen Solubility Parameters Available from: ⟨http://www.hansen-

solubility.com⟩

[54] High-Throughput Membrane Systems Leuven.Available from: ⟨www.html-leuven. be⟩.

[55] J.R. Hwang, S.H. Koo, J.H. Kim, A. Higuchi, T.M. Tak, Effects of casting solution composition on performance of poly(ether sulfone) membrane, J. Appl. Polym. Sci. 60 (1996) 1343–1348.

[56] I. Ahmed, A. Idris, A. Hussain, Z.A.M. Yusof, M. Saad Khan, Influence of Co-solvent concentration on the properties of dope solution and performance of polyether-sulfone membranes, Chem. Eng. Technol. 36 (2013) 1683–1690.

[57] P. Vandezande, L.E.M. Gevers, I.F.J. Vankelecom, Solvent resistant nanofiltration: separating on a molecular level, Chem. Soc. Rev. 37 (2008) 365–405.

[58] H. Strathmann, K. Kock, P. Amar, R.W. Baker, The formation mechanism of asymmetric membranes, Desalination 16 (1975) 179–203.

[59] A. Conesa, T. Gumí, C. Palet, Membrane thickness and preparation temperature as key parameters for controlling the macrovoid structure of chiral activated membranes (CAM), J. Membr. Sci. 287 (2007) 29–40.

[60] B.A. Miller-Chou, J.L. Koenig, A review of polymer dissolution, Prog. Polym. Sci. 28 (2003) 1223–1270.

[61] I. Cabasso, E. Klein, J.K. Smith, Polysulfone hollow fibers. II, Morphol., J. Appl. Polym. Sci. 21 (1977) 165–180.

[62] C.A. Smolders, A.J. Reuvers, R.M. Boom, I.M. Wienk, Microstructures in phase-inversion membranes. Part 1. Formation of macrovoids, J. Membr. Sci. 73 (1992) 259–275.

[63] I. Soroko, Y. Bhole, A.G. Livingston, Environmentally friendly route for the preparation of solvent resistant polyimide nanofiltration membranes, Green. Chem. 13 (2011) 162–168.

[64] S. Hermans, E. Dom, H. Mariën, G. Koeckelberghs, I.F.J. Vankelecom, Efficient synthesis of interfacially polymerized membranes for solvent resistant nanofiltra-tion, J. Membr. Sci. 476 (2015) 356–363.

[65] M.F. Jimenez Solomon, Y. Bhole, A.G. Livingston, High flux membranes for organic solvent nanofiltration (OSN)—Interfacial polymerization with solvent activation, J. Membr. Sci., 423– 424 (2012) 371–382.